Inorg. Chem. **2005**, *44*, 5844–5853

Chemical and Electrochemical Formation of Pseudorotaxanes Composed of Alkyl(ferrocenylmethyl)ammmonium and Dibenzo[24]crown-8

Masaki Horie,† Yuji Suzaki, and Kohtaro Osakada*

Chemical Resources Laboratory, Tokyo Institute of Technology, 4259 Nagatsuta, Midori-ku, Yokohama 226-8503, Japan

Received February 9, 2005

Protonation of *p*-xylylaminomethylferrocene (**1**) and *n*-hexylaminomethylferrocene (**2**) by HCl and NH_4PF_6 forms the ferrocenylmethyl(alkyl)ammonium salt. Inclusion of the compounds by dibenzo[24]crown-8 (DB24C8) produces [2]pseudorotaxanes, $[(DB24C8)(\mathbf{1}–H)]^+(PF_6)$ and $[(DB24C8)(\mathbf{2}–H)]^+(PF_6)$, respectively. X-ray diffraction of the former product indicates an interlocked structure composed of the axis and the macrocyclic molecule. Intermolecular N–H···O and C–H···O interactions and stacking of the aromatic planes are observed. $[(DB24C8)(\mathbf{1}–H)]^+(PF_6)$, in the solid state, is characterized by IR spectroscopy and elemental analyses. A similar reaction of 1,1′-bis(*p*-xylylaminomethyl)ferrocene (**3**) forms a mixture of [2] and [3]pseudorotaxanes, $[(DB24C8)(\mathbf{3}–H_2)]^{2+}(PF_6)_2$ and $[(DB24C8)_2(\mathbf{3}–H_2)]^{2+}(PF_6)_2$. The latter product having two DB24C8 molecules is isolated and characterized by X-ray crystallography. Formation of these pseudorotaxanes in a CD_3CN solution is evidenced by ^1H NMR and mass spectrometry. Electrochemical oxidation of **1**–**3** at 0.4 V (vs Ag^+/Ag) in the presence of TEMPOH (1-hydroxy-2,2,6,6-tetramethylpiperidine) and DB24C8 affords the corresponding pseudorotaxanes. The ESR spectrum of the reaction mixture indicates the formation of a TEMPO radical in high yield. Details of the conversion of the dialkylamino group of the ligand to the dialkylammonium group are investigated by using a flow electrolysis method linked to spectroscopic measurements. The proposed mechanism for the reaction involves the ferrocenium species, formed by initial oxidation, which undergoes electron transfer from nitrogen to the Fe(III) center, producing a cation radical at the nitrogen. Transfer of hydrogen from TEMPOH to the cation radical and inclusion of the resulting dialkylammonium species by DB24C8 yields the pseudorotaxanes.

Introduction

A number of functionalized ferrocenes have been prepared by introduction of the organic groups to the η^5-cyclopentadienyl ligands of ferrocene.[1] The ferrocene derivatives, containing π-conjugated groups in the substituents of the ligand, exhibit both redox of the Fe center and optical properties of the organic group. Smooth electronic communication between the metal and the ligand would enable the cooperative electrochemical and optical performance of these compounds. Anthraquinone substituted by two ferrocenyl groups was reported to undergo electrochemical oxidation, which accompanies change of the absorption spectra.[2] Ferrocene having an azo or azobenzene group at the ligand changes the optical properties depending on the valence of the Fe center.[3] Inclusion of ferrocene and ferrocenium by macrocyclic molecules such as cyclodextrins[4] show different binding constants from each other.[5] Supramolecular systems that cause decomplexation−recomplexation of a guest molecule are proposed on the basis of the above

* To whom correspondence should be addressed. Fax: +81-45-924-5224. E-mail: kosakada@res.titech.ac.jp.

† Present address: Supramolecular Science Laboratory, The Institute of Physical and Chemical Research (RIKEN) 2-1 Hirosawa, Wako, Saitama 351-0198, Japan.

(1) (a) *Ferrocenes*; Togni, A., Hayashi, T., Eds.; VCH: New York, 1995. (b) Nguyen, P.; Gomez-Elipe, P.; Manners, I. *Chem. Rev.* **1999**, *99*, 1515−1548. (c) Colacot, T. J. *Chem. Rev.* **2003**, *103*, 3101−3118, and references therein.

(2) Murata, M.; Yamada, M.; Fujita, T.; Kojima, K.; Kurihara, M.; Kubo, K.; Kobayashi, Y.; Nishihara, H. *J. Am. Chem. Soc.* **2001**, *123*, 12903−12904.

(3) (a) Kurihara, M.; Matsuda, T.; Hirooka, A.; Yutaka, T.; Nishihara, H. *J. Am. Chem. Soc.* **2000**, *122*, 12373−12374. (b) Kurihara, M.; Hirooka, A.; Kume, S.; Sugimoto, M.; Nishihara, H. *J. Am. Chem. Soc.* **2002**, *124*, 8800−8801.

(4) Harada, A.; Takahashi, S. *J. Chem. Soc., Chem. Commun*. **1984**, 645−646.

10.1021/ic050215f CCC: $30.25
Published on Web 07/08/2005

results. A pseudorotaxane composed of a ferrocene derivative, having long chains at the cyclopentadienyl ligands, and cationic paraquat-type macrocycles extrude the ferrocene-containing guest upon electrochemical oxidation.[6] Analogous dethreading−rethreading of the axis molecule in a pseudorotaxane is controlled by pH change of the solution.[7] Rotaxanes that change positions of the cyclic molecules by external stimulus such as change of pH, electrochemical reaction, and photoirradiation are called molecular shuttles.[8,9] An electrochemically driven molecular shuttle was recently prepared by using the ferrocene-containing molecule as the axis molecule.[10] Application of molecular shuttles, proposed by several research groups, covers photoinduced high-speed switching in solution,[11] field effect transistors (FET),[12] and molecular memory in the thin films.[13]

We recently reported that 2-aza[3]ferreocenophanes having an azobenzene group undergo reversible multistep electrochemical oxidation and reduction[14] and proposed electron transfer between the Fe and N atoms at the oxidized state to account for the electrochemical reaction.[15] This electronic communication between the metal and the ligand provides a cationic nitrogen center which would be included by crown ethers to form rotaxanes.[16] In this paper, we report the preparation of pseudorotaxanes containing a ferrocene-substituted ammonium axis from chemical and electrochemical reactions. A part of the work was reported in a preliminarily form.[17]

Scheme 1

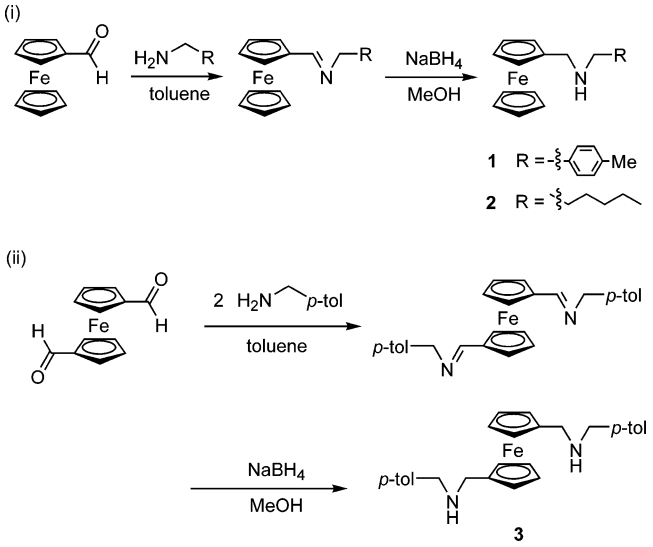

Results and Discussions

Preparation of Pseudorotaxanes and Their Characterization. Scheme 1 summarizes preparation of the aminomethylferrocene derivatives. *p*-Methylbenzylaminomethylferrocene (**1**) and *n*-hexylaminomethylferrocene (**2**) are obtained by condensation of ferrocenecarboxaldehyde with the primary amines followed by $NaBH_4$ reduction of the formed imines. Analogous reaction of 1,1′-ferrocenedicarboxaldehyde yields 1,1′-bis(*p*-xylylaminomethyl)ferrocene (**3**). Treatment of **1**−**3** with $HCl_{(aq)}$ and NH_4PF_6 produces the ferrocene with a dialkylammonium group as the ligand and a PF_6 counteranion, $[\mathbf{1}-H]^+(PF_6)$, $[\mathbf{2}-H]^+(PF_6)$, and $[\mathbf{3}-H_2]^{2+}(PF_6)_2$, as shown in Scheme 2.

Slow addition of Et_2O to a CH_2Cl_2 solution of $[\mathbf{1}-H]^+(PF_6)$ and DB24C8 leads to separation of $[(DB24C8)(\mathbf{1}-H)]^+(PF_6)$ as crystals, as shown in Scheme 3. $[(DB24C8)(\mathbf{3}-H_2)]^{2+}(PF_6)_2$ is isolated similarly by addition of Pr_2O to a CH_2Cl_2/acetone solution of $[\mathbf{3}-H_2]^{2+}(PF_6)_2$ and DB24C8.

The obtained [2] and [3]pseudorotaxanes are characterized by X-ray crystallography and IR spectroscopy. Figure 1 exhibits molecular structures of the [2] and [3]pseudorotaxanes. $[(DB24C8)(\mathbf{1}-H)]^+(PF_6)$ has an interlocked structure with $[\mathbf{1}-H]^+$ threading into the pore of DB24C8.

The NH_2 and CH_2 groups of the axis show short contacts with the oxygen atoms of DB24C8 (NH···O, 2.18 Å and CH···O, 2.35 Å), suggesting the presence of $N^+-H\cdots O$ and $C-H\cdots O$ interactions between the axis and cyclic molecules. The aromatic planes of the axis and cyclic molecules are stacked with each other with a distance between planes of

(5) (a) Isnin, R.; Salam, C.; Kaifer, A. E. *J. Org. Chem.* **1991**, *56*, 35−41. (b) Liu, J.; Alvarez, J.; Ong, W.; Román, E.; Kaifer, A. E. *J. Am. Chem. Soc.* **2001**, *123*, 11148−11154. (c) González, B.; Cuadrado, I.; Alonso, B.; Casado, C. M.; Morán, M.; Kaifer, A. E. *Organometallics* **2002**, *21*, 3544−3551.
(6) Balzani, V.; Becher, J.; Credi, A.; Nielsen, M. B.; Raymo, F. M.; Stoddart, J. F.; Talarico, A. M.; Venturi, M. *J. Org. Chem.* **2000**, *65*, 1947−1956.
(7) Ashton, P. R.; Ballardini, R.; Balzani, V.; Fyfe, M. C. T.; Gandolfi, M. T.; Martínez-Díaz, M.-V.; Morosini, M.; Schiavo C.; Shibata, K.; Stoddart, J. F.; White, A. J. P.; Williams, D. J. *Chem. Eur. J.* **1998**, *4*, 2332−2341.
(8) (a) Anelli, P. L.; Spencer, N.; Stoddart, J. F. *J. Am. Chem. Soc.* **1991**, *113*, 5131−5133. (b) Bissell, R. A.; Córdova, E.; Kaifer, A. E.; Stoddart, J. F. *Nature* **1994**, *369*, 133−137. (c) Balzani, V.; Credi, A.; Mattersteig, G.; Matthews, O. A.; Raymo, F. M.; Stoddart, J. F.; Venturi, M.; White, A. J. P.; Williams, D. J. *J. Org. Chem.* **2000**, *65*, 1924−1936. (d) Altieri, A.; Gatti, F. G.; Kay, E. R.; Leigh, D. A.; Martel, D.; Paolucci, F.; Slawin, A. M. Z.; Wong, J. K. Y. *J. Am. Chem. Soc.* **2003**, *125*, 8644−8654.
(9) (a) Ashton, P. R.; Ballardini, R.; Balzani, V.; Baxter, I.; Credi, A.; Fyfe, M. C. T.; Gandolfi, M. T.; Gómez-López, M.; Martínez-Díaz, M.-V.; Piersanti, A.; Spencer. N.; Stoddart, J. F.; Venturi, M.; White, A. J. P.; Williams, D. J. *J. Am. Chem. Soc.* **1998**, *120*, 11932-11942. (b) Murakami, H.; Kawabuchi, A.; Kotoo, K.; Kunitake, M.; Nakashima, N. *J. Am. Chem. Soc.* **1997**, *119*, 7605−7606. (c) Bottari, G.; Leigh, D. A.; Pérez, E. M. *J. Am. Chem. Soc.* **2003**, *125*, 13360−13361. (d) Pérez, E. M.; Dryden, D. T. F.; Leigh, D. A.; Teobaldi, G.; Zerbetto, F. *J. Am. Chem. Soc.* **2004**, *126*, 12210−12211.
(10) Kihara, N.; Hashimoto, M.; Takata, T. *Org. Lett.* **2004**, *6*, 1693−1696.
(11) Brouwer, A. M.; Frochot, C.; Gatti, F. G.; Leigh, D. A.; Mottier, L.; Paolucci, F.; Roffia, S.; Wurpel, G. W. H. *Science* **2001**, *291*, 2124−2128.
(12) (a) Joachim, C.; Gimzewski, J. K.; Aviram, A. *Nature* **2000**, *408*, 541−548. (b) Cavallini, M.; Biscarini, F.; León, S.; Zerbetto, F.; Bottari, G.; Leigh, D. A. *Science* **2003**, *299*, 531.
(13) Collier, C. P.; Wong, E. W.; Belohradsky, M.; Raymo, F. M.; Stoddart, J. F.; Kuekes, P. J.; Williams, R. S.; Heath, J. R. *Science* **1999**, *285*, 391−394.
(14) (a) Horie, M.; Sakano, T.; Osakada, K.; Nakao, H. *Organometallics* **2004**, *23*, 18−20. (b) Sakano, T.; Horie, M.; Osakada, K.; Nakao, H. *Eur. J. Inorg. Chem.* **2005**, *4*, 644−652.
(15) Sakano, T.; Horie, M.; Osakada, K.; Nakao, H. *Bull. Chem. Soc. Jpn.* **2001**, *74*, 2059−2065.
(16) For recent reviews of ammonium−crown ether rotaxane, see: (a) Raymo, F. M.; Stoddart, J. F. *Chem. Rev.* **1999**, *99*, 1643−1663. (b) Balzani, V.; Credi, A.; Raymo, F. M.; Stoddart, J. F. *Angew. Chem., Int. Ed.* **2000**, *39*, 3348−3391. (c) Balzani, V.; Venturi, M.; Credi, A. *Molecular Devices and Machines − A Journey into the Nano World*; Wiley-VCH: Weinheim, 2003.
(17) Horie, M.; Suzaki, Y.; Osakada, K. *J. Am. Chem. Soc.* **2004**, *126*, 3684−3685.

Scheme 2

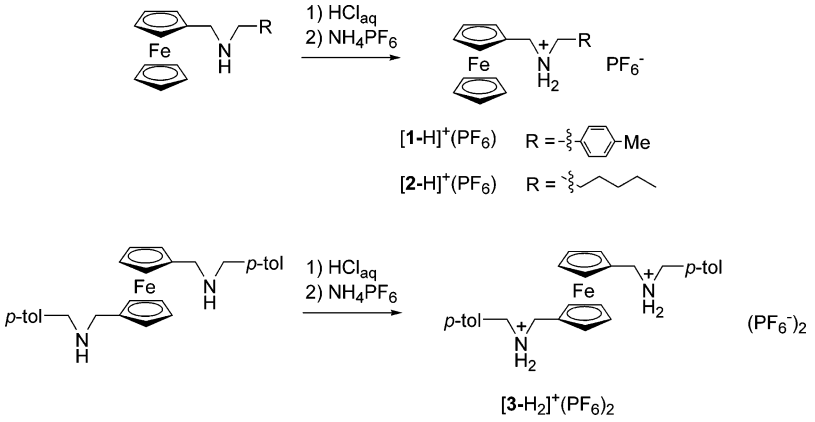

Scheme 3

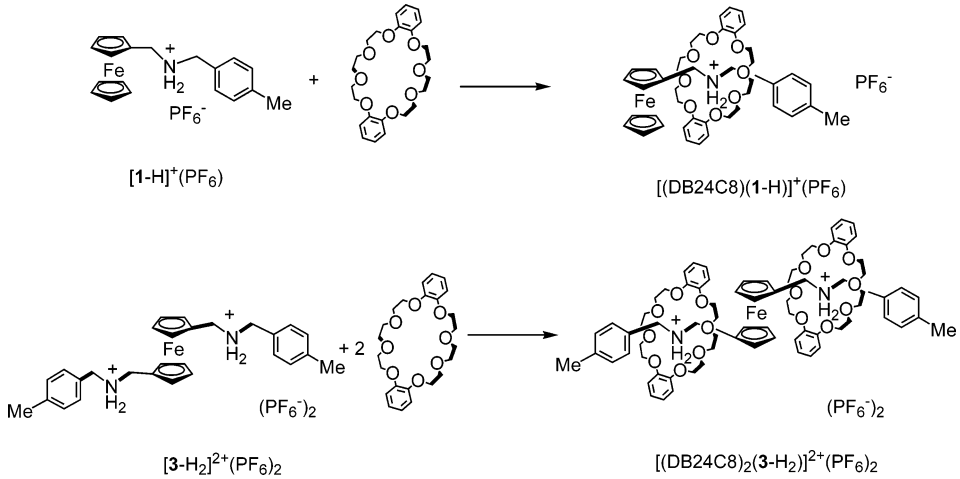

3.34 Å. [(DB24C8)$_2$(**3**−H$_2$)]$^{2+}$(PF$_6$)$_2$ contains two DB24C8 molecules which include the cationic groups attached to the cyclopentadienyl ligands. The bulky pseudorotaxane groups are oriented to avoid steric repulsion.

Figure 2 compares the IR spectra of [(DB24C8)(**1**−H)]$^+$-(PF$_6$), [**1**−H]$^+$(PF$_6$), DB24C8, and a mixture of [**1**−H]$^+$(PF$_6$) and DB24C8. Peaks due to asymmetric and symmetric vibration of the NH$_2$ group of [**1**−H]$^+$(PF$_6$) are observed at 3266 and 3233 cm^{-1}, respectively.

The ν_{N-H} positions of [(DB24C8)(**1**−H)]$^+$(PF$_6$) are shifted to lower wavenumber by 100 cm^{-1} (ν_{N-H} = 3166 cm^{-1}) and 166 cm^{-1} (ν_{N-H} = 3067 cm^{-1}) from that of [**1**−H]$^+$(PF$_6$), respectively, indicating weaker N−H bonds of the pseudorotaxane than those in the free axis molecule due to N$^+$−H···O hydrogen bonds.

Thermal properties of the rotaxanes and the pseudorotaxanes in the solid state are of interest, although the number of the studies on this subject is small.[18] TGA (thermal gravimetric analysis) of [(DB24C8)(**1**−H)]$^+$(PF$_6$) shows 5% weight loss at 237 °C, which is between those of [**1**−H]$^+$-(PF$_6$) (217 °C) and DB24C8 (309 °C) (Figure 3).

An equimolar mixture of [**1**−H]$^+$(PF$_6$) and DB24C8 undergoes similar weight decrease, suggesting that [(DB24C8)-(**1**−H)]$^+$(PF$_6$) is dissociated to DB24C8 and [**1**−H]$^+$(PF$_6$) on heating in the solid state. DSC (differential scanning calorimetric) measurement of [(DB24C8)(**1**−H)]$^+$(PF$_6$) shows endothermic and exothermic peaks at 125 °C on heating and 114 °C on cooling, respectively. The differential enthalpy of the phase transition is ΔH = 1.8 kcal mol^{-1} at 125 °C. The temperature of this phase transition of [(DB24C8)(**1**−H)]$^+$(PF$_6$) differs from those of [**1**−H]$^+$(PF$_6$) (T_{end} = 188 °C) and of DB24C8 (T_{end} = 104 °C, T_{exo} = 79 °C).

Dissolution of an equimolar mixture of [**1**−H]$^+$(PF$_6$) and DB24C8 in CD$_3$CN (10 mM for each compound) gives rise to the ^{1}H NMR peaks of CH$_2$N hydrogens of [(DB24C8)-(**1**−H)]$^+$(PF$_6$) at 4.37 and 4.53 ppm and those of [**1**−H]$^+$-(PF$_6$) at 4.04 and 4.06 ppm. Chemical exchange between the pseudorotaxane and its free axis should take place in the solution, although it is slower than the NMR time scale. Downfield shifts of the CH$_2$N hydrogen peaks were reported for pseudorotaxanes composed of DB24C8 and dibenzylammonium cations.[19] The ratio of [**1**−H]$^+$(PF$_6$) to [(DB24C8)-(**1**−H)]$^+$(PF$_6$) is determined to be 49:51 from the peak intensity of the cyclopentadienyl hydrogens. Formation of [(DB24C8)(**2**−H)]$^+$(PF$_6$) from [**2**−H]$^+$(PF$_6$) and DB24C8 in CD$_3$CN (10 mM for each compound) is confirmed by the ^{1}H NMR spectroscopy. The CH$_2$N hydrogen signal of [**2**−H]$^+$(PF$_6$) (2.90 ppm) is at a higher-field position than the corresponding hydrogens of [(DB24C8)(**2**−H)]$^+$(PF$_6$)

(18) Gibson, H. W.; Liu, S.; Lecavalier, P.; Wu, C.; Shen, Y. X. *J. Am. Chem. Soc.* **1995**, *117*, 852−874.

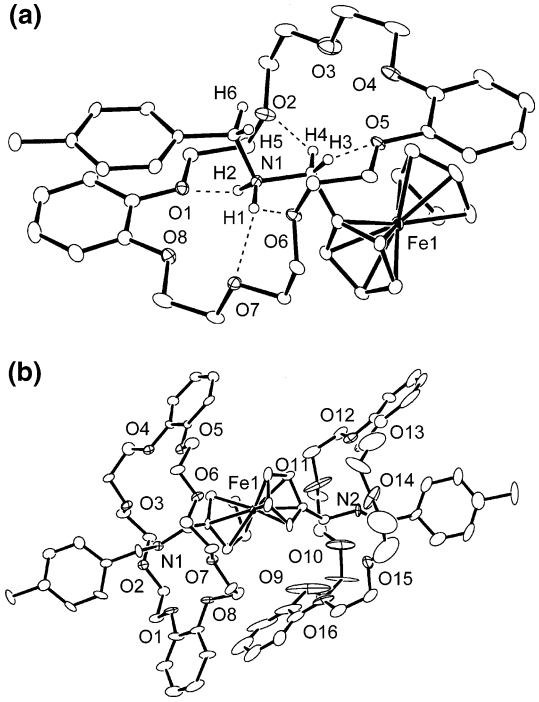

Figure 1. ORTEP drawing of (a) $[(DB24C8)(\mathbf{1}-H)]^+(PF_6)$ and (b) $[(DB24C8)_2(\mathbf{3}-H_2)]^{2+}(PF_6)_2$ with 30% ellipsoidal plotting. PF_6^- anions are omitted. Positions of the hydrogen atoms are obtained by calculation.

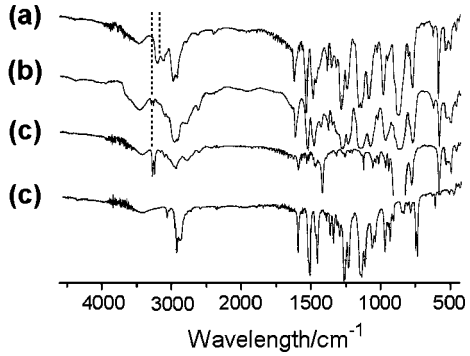

Figure 2. IR spectra of (a) $[(DB24C8)(\mathbf{1}-H)]^+(PF_6)$, (b) mixture of $[\mathbf{1}-H]^+(PF_6)$ and DB24C8, (c) $[\mathbf{1}-H]^+(PF_6)$, and (d) DB24C8.

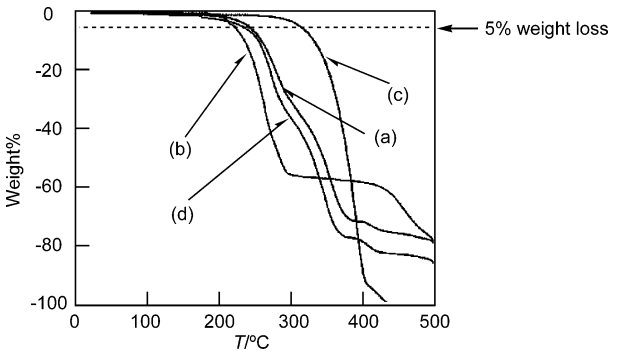

Figure 3. TGA curves of (a) $[(DB24C8)(\mathbf{1}-H)]^+(PF_6)$, (b) $[\mathbf{1}-H]^+(PF_6)$, (c) DB24C8, and (d) an equimolar mixture of $[\mathbf{1}-H]^+(PF_6)$ and DB24C8. Heating rate = 10 °C min^{-1}.

(3.32 ppm). The ratio of $[\mathbf{2}-H]^+(PF_6)$ and $[(DB24C8)(\mathbf{2}-H)]^+(PF_6)$ is 1.0:1.0 in the solution.

Mixing $[\mathbf{3}-H_2]^{2+}(PF_6)_2$ and DB24C8 in CD_3CN forms [2] and [3]pseudorotaxanes whose ratio depends on the ratio of the axis and cyclic molecules employed. Figure 4(a) shows

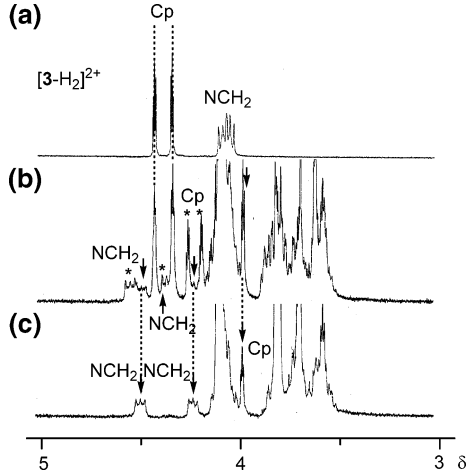

Figure 4. ^1H NMR spectra in CD_3CN at room temperature (300 MHz). (a) $[\mathbf{3}-H_2]^{2+}(PF_6)_2$, (b) a mixture of $[\mathbf{3}-H_2]^{2+}(PF_6)_2$ and DB24C8 in a 1:1 molar ratio (10 mM for each compound), and (c) a mixture of $[\mathbf{3}-H_2]^{2+}(PF_6)_2$ (10 mM) and DB24C8 (50 mM) in a 1:5 molar ratio.

the ^1H NMR spectrum of $[\mathbf{3}-H_2]^{2+}(PF_6)_2$ which exhibits the cyclopentadienyl hydrogens at 4.41 and 4.32 ppm and CH_2-N^+ hydrogens at 4.01−4.09 ppm.

The ^1H NMR spectrum of a mixture of DB24C8 and $[\mathbf{3}-H_2]^{2+}(PF_6)_2$ (10 mM for each compound) (Figure 4(b)) exhibits the signals of the CH_2-N^+ hydrogens at lower-field positions than those of the axis molecule (4.56, 4.48, 4.38, and 4.21 ppm). The signals at 4.48 and 4.21 ppm are assigned to $[(DB24C8)_2(\mathbf{3}-H_2)]^{2+}(PF_6)_2$, while the signals at 4.56 and 4.38 ppm are due to $[(DB24C8)(\mathbf{3}-H_2)]^{2+}(PF_6)_2$. The spectrum of a solution of DB24C8 (50 mM) and $[\mathbf{3}-H_2]^{2+}(PF_6)_2$ (10 mM) displays two signals for the CH_2-N^+ hydrogens (4.48 and 4.21 ppm) (Figure 4(c)). The signal at 3.96 ppm observed in Figure 4(b) and (c) is due to cyclopentadienyl hydrogens of $[(DB24C8)_2(\mathbf{3}-H_2)]^{2+}(PF_6)_2$, while Figure 4(b) shows the signals of $[(DB24C8)(\mathbf{3}-H_2)]^{2+}(PF_6)_2$ at 4.56 and 4.38 ppm. The ratio among $[\mathbf{3}-H_2]^{2+}(PF_6)_2$, $[(DB24C8)(\mathbf{3}-H_2)]^{2+}(PF_6)_2$, and $[(DB24C8)_2(\mathbf{3}-H_2)]^{2+}(PF_6)_2$ is determined to be 4.0:4.2:1.1 from the peak-area ratio of Cp hydrogens.

The cyclic voltammogram of $[(DB24C8)(\mathbf{1}-H)]^+(PF_6)$ in CH_3CN shows reversible redox at $E_{1/2} = 0.23$ V (vs Ag^+/Ag). $[(DB24C8)(\mathbf{1}-H)]^+(PF_6)$ up to 0.4 V does not show any other oxidation reaction. The positive charge of the pseudorotaxane renders the potential at a more positive position than **1**.[5,20,21] The redox potential is the same as that of $[\mathbf{1}-H]^+(PF_6)$. It is contrasted with the observed shielding

(19) (a) Ashton, P. R.; Campbell, P. J.; Chrystal, E. J. T.; Glinke, P. T.; Menzer, S.; Philp, D.; Spencer, N.; Stoddart, J. F.; Tasker, P. A.; Williams, D. J. *Angew. Chem., Int. Ed. Engl.* **1995**, 1865−1869. (b) Ashton, P. R.; Chrystal, E. J. T.; Glink, P. T.; Menzer, S.; Schiavo, C.; Spencer, N.; Stoddart, J. F.; Tasker, P. A.; White, A. J. P.; Williams, D. J. *Chem. Eur. J.* **1996**, *2*, 709−728. (c) Ashton, P. R.; Fyfe, M. C. T.; Hickingbottom, S. K.; Stoddart, J. F.; White, A. J. P.; Williams, D. J. *J. Chem. Soc., Perkin Trans. 2* **1998**, 2117−2128. (d) Chang, T.; Heiss, A. M.; Cantrill, S. J.; Fyfe, M. C. T.; Pease, A. R.; Rowan, S. J.; Stoddart, J. F.; Williams, D. J. *Org. Lett.* **2000**, *2*, 2943−2946. (e) Williams, A. R.; Northrop, B. H.; Houk, K. N.; Stoddart, J. F.; Williams, D. J. *Chem. Eur. J.* **2004**, *10*, 5406−5421.

(20) (a) Alvarez, J.; Kaifer, A. E. *Organometallics* **1999**, *18*, 5733−5734. (b) Alvarez, J.; Ren, T.; Kaifer, A. E. *Organometallics* **2001**, *20*, 3543−3549.

Scheme 4

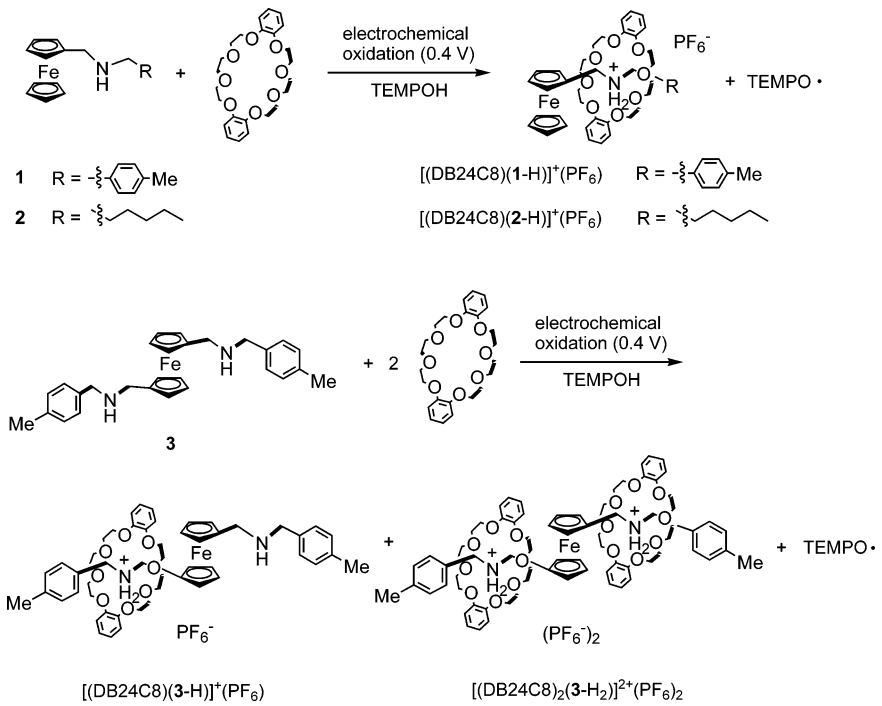

effect of the macrocyclic component in the interlocked structure of the rotaxane composed of a ferrocene-containing axis molecule and DB24C8.[10]

Formation of Pseudorotaxane Induced by Electrochemical Oxidation. Electrochemical oxidation of **1** and **2** at 0.4 V (vs Ag^+/Ag) in the presence of DB24C8 and TEMPOH produces the [2]pseudorotaxanes composed of the ferrocene derivative, with the dialkylammonium group and DB24C8, as shown in Scheme 4.

A mixture of the [2] and [3]pseudorotaxanes, $[(DB24C8)(\mathbf{3}-H)]^+$ and $[(DB24C8)_2(\mathbf{3}-H_2)]^{2+}$, is obtained from the oxidation of **3** at the same potential in the presence of TEMPOH and DB24C8. A CH_3CN solution of a mixture of **1**, *n*-Bu_4NPF_6, DB24C8, and TEMPOH does not produce a pseudorotaxane without electrochemical oxidation.

Figure 5(a) depicts the FAB mass spectrum after electrochemical oxidation of **1** at 0.4 V in the presence of DB24C8 and TEMPOH.

A peak at $m/z = 768$ is assigned to the cationic part of $[(DB24C8)(\mathbf{1}-H)]^+(PF_6)$. Flow electrolysis of **2** in the presence of TEMPOH and DB24C8 at 0.4 V leads to the formation of $[(DB24C8)(\mathbf{2}-H)]^+$, which shows a peak at $m/z = 748$ in the mass spectrum (Figure 5(b)). The CH_3CN solution after flow electrolysis of **3** in the presence of TEMPOH and DB24C8 at 0.4 V shows the FAB mass peak at $m/z = 674$ corresponding to the dicationic [3]pseudorotaxane, $[(DB24C8)_2(\mathbf{3}-H_2)]^{2+}$ and that at $m/z = 901$ due to the monocationic [2]pseudorotaxane, $[(DB24C8)(\mathbf{3}-H)]^+$ (Figure 5(c)). These reactions convert TEMPOH into the TEMPO radical. Figure 6(a) displays the ESR spectrum of the solution, obtained by electrochemical oxidation of **1** and subsequent addition of TEMPOH. The three peaks are assigned to the TEMPO radical by comparison with the standard sample (Figure 6(b)). The intensity of the produced TEMPO radical is determined as 92% of the initially charged TEMPOH.[22] The solution without electrochemical oxidation gives the signal with a much smaller intensity (Figure 6(c)).

Formation of the pseudorotaxanes indicates that the electrochemical oxidation in the presence of TEMPOH

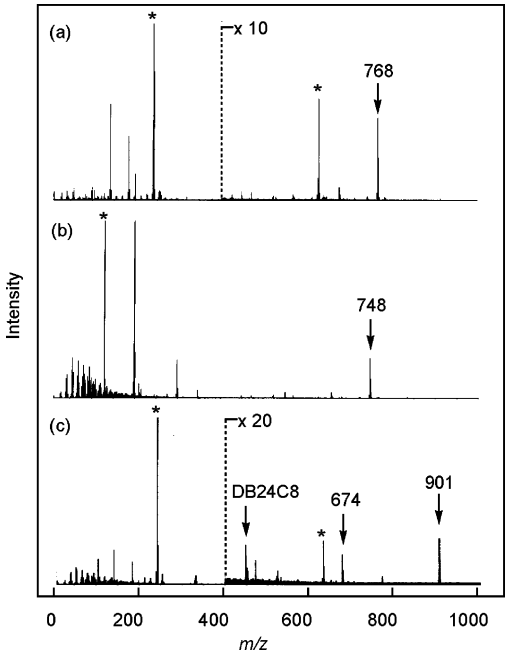

Figure 5. FAB mass spectra of (a) $[(DB24C8)(\mathbf{1}-H)]^+$, (b) $[(DB24C8)(\mathbf{2}-H)]^+$, and (c) $[(DB24C8)(\mathbf{3}-H)]^+$ and $[(DB24C8)_2(\mathbf{3}-H_2)]^{2+}$. The pseudorotaxanes formed by the electrochemical oxidation of the axis molecules at 0.4 V by using of flow electrolysis system are applied to measurement. A mixture of glycerol and *m*-nitrobenzyl alcohol was used as the matrix. Peaks with asterisks are due to the compounds used as the matrixes.

(21) (a) Menger, F. M.; Sherrod, M. J. *J. Am. Chem. Soc.* **1988**, *110*, 8606−8611. (b) Matsue, T.; Evans, D. H.; Osa, T.; Kobayashi, N. *J. Am. Chem. Soc.* **1985**, *107*, 3411−3417.

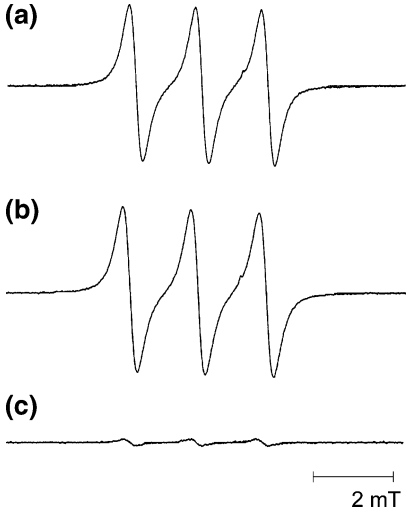

Figure 6. ESR spectra of (a) **1** (1.0 mM) and *n*-Bu_4NPF_6 (1.0 mM) after flow electrolysis at 0.4 V and addition of TEMPOH (1.0 mM), (b) TEMPO (1.0 mM), and (c) a mixture of **1** (1.0 mM), *n*-Bu_4NPF_6 (1.0 mM) and TEMPOH (1.0 mM). $g = 2.0059$.

induces protonation of the dialkylamino group of **1**−**3** to afford the ferrocene derivatives with the dialkylammonium group at the ligands. The reactions without addition of TEMPOH take place much more slowly but produce similar products. Electrochemical and spectroscopic measurements of the reaction mixtures are conducted in order to elucidate the detailed mechanism of the protonation. Cyclic and linear sweep voltammograms during the electrochemical oxidation of **1** (2.0 mM) indicate that the quantitative one-electron oxidation at 0.40 V (vs Ag^+/Ag) converts the ferrocenylene group into ferrocenium in >98% yield.[23] The presence of DB24C8 does not influence this reaction at all.[9a]

The products of flow electrolysis of **1** (2.0 mM) in the presence of H_2O (2.0 mM) and *n*-Bu_4NPF_6 at 0.4 V were analyzed by ^1H NMR and absorption spectra. The ^1H NMR signals of the CH_2-N^+ hydrogens (4.04 and 4.06 ppm) are at the same positions as those of $[\mathbf{1}-H]^+(PF_6)$ prepared by protonation of **1**, as shown in Figure 7(a) and (b).

The other peak positions are identical to each other except for the peaks of the electrolyte in the electrochemically prepared $[\mathbf{1}-H]^+(PF_6)$. Addition of DB24C8 to the product yields the pseudorotaxane $[(DB24C8)(\mathbf{1}-H)]^+$, which gives rise to the ^1H NMR signals at 4.37 and 4.53 ppm.

The absorption spectra of the solution during the electrochemical oxidation without addition of TEMPOH show immediate formation of a peak at 630 nm and its gradual decrease. Scheme 5 displays a plausible pathway of the reaction converting **1** into $[\mathbf{1}-H]^+$. Initial electrochemical oxidation of the Fe center takes place rapidly to form a ferrocenium intermediate (i). Subsequent electron transfer from nitrogen to Fe(III) and intermolecular hydrogen transfer from other compounds afford the product (ii). Since TEMPOH is a good source of hydrogen radical, reaction (ii) is accelerated by addition of TEMPOH.

(22) (a) Keana, J. F. W. *Chem. Rev.* **1978**, *78*, 37−64. (b) Roth, J. P.; Yoder, J. C.; Won, T.-J.; Mayer, J. M. *Science* **2001**, *294*, 2524−2526.

(23) Nakao, H.; Hayashi, H.; Okita, K. *Anal. Sci.* **2001**, *17*, 545−549.

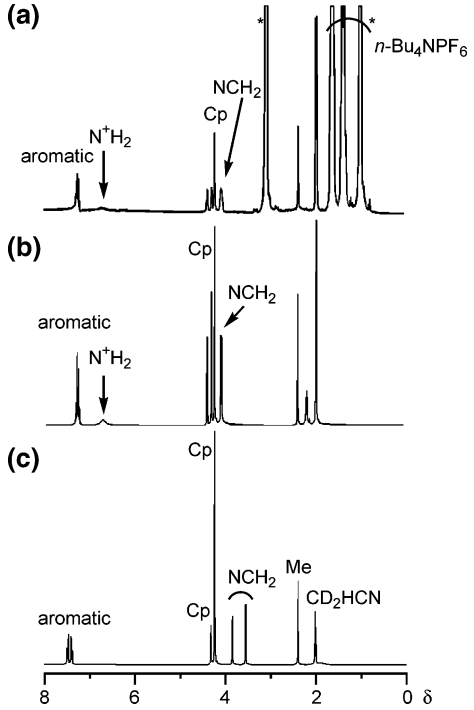

Figure 7. ^1H NMR spectra of (a) $[\mathbf{1}-H]^+(PF_6)$ (electrochemically hydrogenated), (b) $[\mathbf{1}-H]^+(PF_6)$ (chemically protonated), and (c) **1** in CD_3CN (300 MHz).

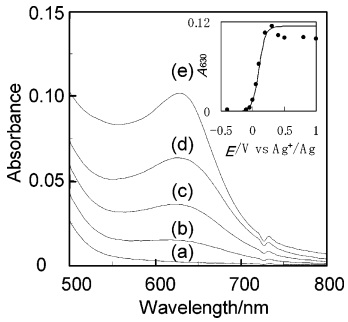

Figure 8. Absorption spectra of **1** in the presence of DB24C8 in a CH_3CN solution of 10 mM *n*-Bu_4NPF_6. $[\mathbf{1}]_0 = 2.0$ mM, $[DB24C8]_0 = 4.0$ mM. Spectra measured immediately after the electrolysis at (a) −0.4 (vs Ag^+/Ag), (b) 0, (c) 0.05, (d) 0.1, and (e) 0.40 V.

Scheme 5

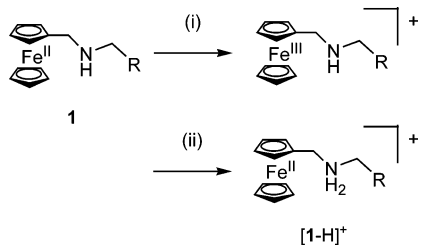

Figure 8 shows the spectra of the solution soon after electrochemical oxidation of a mixture of **1** and DB24C8 (1:2 molar ratio) at constant potentials (−0.4−1.0 V).

The peak at 630 nm, whose intensity increases with an increase of the applied potential, E_{app}, is assigned to the ferrocenium ion on the basis of the characteristic peak position.[24] Applying of the Nernst equation ($E_{app} = E° +$

(24) Winter, R. F.; Wolmershäuser, G. *J. Organomet. Chem.* **1998**, *570*, 201−218.

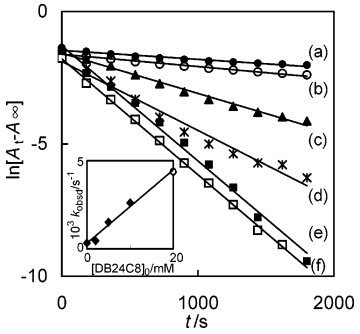

Figure 9. Pseudo-first-order plots of consumption of ferricinium ion of **1** in the presence of DB24C8 of (a) 0 ($k_{obsd} = 3.4 \times 10^{-4}$ s^{-1}), (b) 2.0 ($k_{obsd} = 4.6 \times 10^{-4}$ s^{-1}), (c) 5 ($k_{obsd} = 1.5 \times 10^{-3}$ s^{-1}), (d) 10 ($k_{obsd} = 2.6 \times 10^{-3}$ s^{-1}), (e) 20 ($k_{obsd} = 4.4 \times 10^{-3}$ s^{-1}), and (f) 20 mM with H_2O ($k_{obsd} = 4.4 \times 10^{-3}$ s^{-1}). Change in the observed rate constants depending on the DB24C8 concentration is in inset.

(RT/nF) ln([Ox]/[Red]), $E°$ = the formal oxidation potential), by assuming an equilibrium between the oxidized and reduced species, gave $E° = 0.10$ V and $n = 0.5$. The n value, which is much smaller that expected for one-electron oxidation (1.0), indicates that a irreversible chemical reaction of the oxidized species also takes place at this potential.

The above solutions undergo gradual decrease in the peak intensity at 630 nm, while addition of TEMPOH to the solution (2.0 mM) results in disappearance of the peak within 2 s. These reactions correspond to the conversion of the ferrocenium into the ferrocene bonded to the dialkylammonium group (Scheme 5(ii)). Figure 9 displays first-order plots of decrease in the peak intensity at various concentrations of DB24C8 in the absence of TEMPOH. The observed rate constants, k_{obsd}, vary from 3.4×10^{-4} ([DB24C8]$_0 = 0$ mM) to 4.4×10^{-3} s^{-1} ([DB24C8]$_0 = 20$ mM).

Increase of the concentration of DB24C8 increases the observed rate constants, indicating that DB24C8 enhances the conversion of the ferrocenium with dialkylamine group into the ferrocene having a dialkylammonium group. The reaction in the presence of [15]crown-5 (20 mM) instead of DB24C8 proceeds with $k_{obsd} = 2.4 \times 10^{-3}$ s^{-1}, which is larger than that for the reaction without addition of the crown ethers (3.4×10^{-4} s^{-1}). Thus, the crown ether with a too-small cavity to include the dialkylammonium group also enhances the reaction.

Scheme 6 summarizes the mechanism that accounts for the above results for electrochemical oxidation of **1** into [**1**−H]$^+$(PF_6) and its pseudorotaxane. One-electron oxidation of **1** forms the ferrocenium species **A** containing an Fe(III) center, as shown in (i). **A** is in fast equilibrium with **B**, having an Fe(II) center and a cation radical at the N atom via electron transfer between the Fe and N atoms.

Similar electron transfer between N and Fe(III) atoms of aminoalkylferrocenium species is proposed to explain the electrochemical behavior of 2-aza[3]ferrocenophanes and oligoferrocenes with Fe−CH_2−NR−CH_2−Fe groups.[15,20] The absorption spectrum in Figure 8(e) shows a similar peak intensity for [Fe(Cp_2)]$^+$(PF_6) (approximately 86%), indicating that the equilibrium is shifted to the formation of **A** with the Fe(III) center. TEMPOH transfers a hydrogen radical to the cation radical at the nitrogen of **B** to produce a secondary

Scheme 6

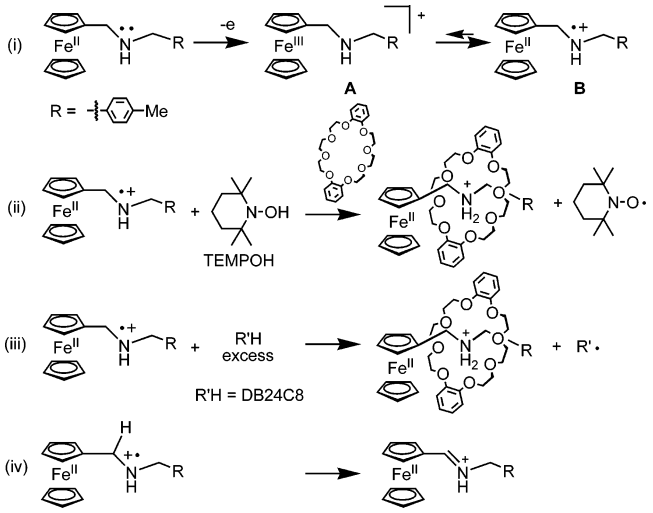

ammonium cation and a TEMPO radical. The formed dialkylammonium group undergoes inclusion by DB24C8 immediately to afford the pseudorotaxane (ii). In the absence of TEMPOH, the intermediate **B** is hydrogenated by the CH_2 group of DB24C8 much more slowly than the reaction with TEMPOH to produce the ferrocene-containing dialkylammonium group. Since the mass spectra of the pseudorotaxanes formed by the reactions without TEMPOH give rise to the peak composed of the axis molecule and DB24C8, the cyclic compound whose hydrogen is abstracted does not form the rotaxane with the cationic axis molecule. Enhancement of the reaction by [15]crown-5 indicates that the hydrogen transfer from the crown ether to the nitrogen cation radical does not require inclusion of the cyclic compound to the cation radical species. The reaction without addition of TEMPOH and DB24C8 causes intramolecular C−H hydrogen abstraction from the aminomethyl cation radical to produce the imminium [−CH=N$^+$−] cation ($m/z = 319$ observed by FAB mass spectroscopy).

In summary, we synthesized new [2] and [3]pseudorotaxanes containing ferrocenyl groups on the axis molecule and DB24C8 and identified them well in the solid state and in solution. Electrochemical oxidation coupled with the transfer of a hydrogen atom from a hydrogen source such as TEMPOH provides the pseudorotaxanes with DB24C8. Electron transfer between the Fe and N atoms plays an important role for formation of the dialkylammonium from the dialkylamine group.

Experimental Section

General Methods. 1[25] and 1,1′-ferrocenedicarboxaldehyde[26] were prepared according to the literature methods. DB24C8 and ferrocenecarboxaldehyde were purchased from Tokyo Kasei Kogyo Co., Ltd. and Strem Chemicals. ^{1}H and ^{13}C{^{1}H} NMR spectra were recorded on JEOL EX-400 and Varian Mercury 300 spectrometers. The chemical shifts were referenced with the solvent peaks ($CHCl_3$, $\delta_H = 7.24$; CD_2HCN, $\delta_H = 1.93$; $CDCl_3$, $\delta_C = 77.0$; and CD_3CN,

(25) Hess, A.; Brosch, O.; Weyhermüller, T.; Metzler-Nolte, N. *J. Organomet. Chem.* **1999**, *589*, 75−84.
(26) Bastin, S.; Agbossou-Niedercorn, F.; Brocard, J.; Pelinski, L. *Tetrahedron: Asymmetry* **2001**, *12*, 2399−2408.

δ_C = 1.30). IR spectra were recorded on Shimadzu FT/IR-8100 spectrometers. Elemental analyses were carried out with a Yanaco MT-5 CHN autorecorder. Melting point determinations were carried out with a Yanagimoto Seisakusho Micro Melting Point Apparatus. TGA and DSC analyses were conducted on Seiko TG/DTA6200R and DSC6200S, respectively. FAB mass spectra were obtained with JEOL JMS-700 using glycerol or *m*-nitrobenzyl alcohol as the matrix. ESR spectra were recorded on a JEOL RE3X spectrometer. Cyclic voltammetry (CV) was measured in CH_3CN solutions containing 10 mM *n*-Bu_4NPF_6 with ALS electrochemical analyzer Model-600A. The measurement was carried out in a standard one-compartment cell under inert gas equipped with a Ag^+/Ag reference electrode, a platinum-wire counter electrode, and a platinum-disk working electrode (ID, 1.6 mm). A combination of flow through an electrolysis cell, a peristaltic pump SMP-11 at 0.7 mL min^{-1}, and a JASCO V-530 UV/VIS spectrometer was used for the linear sweep voltammetry and the spectroelectrochemical measurements in situ.[23]

Preparation of (*n*-Hexylamino)methylferrocene (2). A toluene solution (80 mL) containing ferrocenecarboxaldehyde (2.13 g, 10.0 mmol) and *n*-hexylamine (1.02 g, 10.1 mmol) was stirred for 24 h at 80 °C in the presence of MS4A (4 Å molecular sieves). MS4A was removed by filtration, and the filtrate was evaporated to give *n*-hexyliminomethylferrocene as a brown oil which is used without further purification [^{1}H NMR spectrum (300 MHz, $CDCl_3$, r. t.): δ 0.92 (m, 3H, CH_3), 1.32−1.35* (6H, CH_2), 1.65 (m, 2H, CH_2), 3.46 (2H, NCH_2), 4.19 (s, 5H, C_5H_5), 4.36 (s, 2H, C_5H_4), 4.64 (s, 2H, C_5H_4), 8.11 (s, 1H, NCH). $^{13}C\{^1H\}$ NMR spectrum (75.5 MHz, $CDCl_3$, r. t.): δ 14.0 (CH_3), 22.5 (CH_2), 26.9 (CH_2), 30.8 (CH_2), 31.6 (CH_2), 61.9 (NCH_2), 68.2 (C_5H_4 or C_5H_5), 68.9 (C_5H_4 or C_5H_5), 70.1 (C_5H_4 or C_5H_5), 80.7 (C_5H_4), 160.4 (NCH).]. The above product was dissolved in THF/MeOH (50 mL:50 mL) at room temperature. $NaBH_4$ (766 mg, 20.5 mmol) was added to the solution, and the mixture was stirred for 2 h at room temperature. An extra portion of $NaBH_4$ (720 mg, 19.0 mmol) was added to the reaction mixture. Stirring was continued for 12 h before the product being quenched with 1 N HCl (100 mL). After evaporation of the solvent, the remaining solid was partitioned between 2 N KOH and CH_2Cl_2. The organic extract was dried over $MgSO_4$, filtered, and concentrated under reduced pressure to give **2** as a brown oil (2.31 g, 7.75 mmol, 78%). Anal. Calcd. For $C_{17}H_{25}NFe$: C, 68.24; H, 8.42; N, 4.68. Found: C, 68.76; H, 8.07; N, 4.61. ^{1}H NMR spectrum (300 MHz, $CDCl_3$, r. t.): δ 0.86 (t, 3H, CH_3, *J* (HH) = 7 Hz), 1.26−1.28* (6H, CH_2), 1.46 (m, 2H, CH_2), 2.60 (t, 2H, NCH_2, *J* (HH) = 8 Hz), 3.48 (s, 2H, NCH_2), 4.08 (m, 2H, C_5H_4), 4.10 (s, 5H, C_5H_5), 4.16 (m, 2H, C_5H_4). $^{13}C\{^1H\}$ NMR spectrum (75.5 MHz, $CDCl_3$, r. t.): δ 14.0 (CH_3), 22.6 (CH_2), 27.1 (CH_2), 30.0 (CH_2), 31.8 (CH_2), 49.1 (NCH_2), 49.7 (NCH_2), 67.7 (C_5H_4 or C_5H_5), 68.2−68.4* (2C, C_5H_4 or C_5H_5), 68.4 (C_5H_4 or C_5H_5). The peaks with asterisks are overlapped significantly with other signals.

Preparation of 1,1′-Bis(*p*-xylylaminomethyl)ferrocene (Fc-imine). A solution of 1,1′-ferrocenedicarboxaldehyde (1.21 g, 5.00 mmol) and *p*-methylbenzylamine (1.21 g, 9.99 mmol) in toluene (80 mL) was stirred for 3 days at 80 °C in the presence of MS4A. MS4A was removed by the filtration, and the filtrate was evaporated to give **Fc-imine** as a redbrick solid, which was purified by recrystallization from Et_2O (1.63 g, 3.64 mmol, 73%). Anal. Calcd. for $C_{28}H_{28}N_2Fe$: C, 75.00; H, 6.29; N, 6.25. Found: C, 74.60; H, 6.48; N, 6.04. ^{1}H NMR (300 MHz, CD_3CN, r. t.): δ 2.31 (s, 6H, CH_3), 4.33 (m, 4H, C_5H_4), 4.54 (s, 4H, CH_2), 4.63 (m, 4H, C_5H_4), 7.14 (t, 4H, *o*-C_6H_4 or *m*-C_6H_4, *J* (HH) = 8 Hz), 7.16 (t, 4H, *o*-C_6H_4 or *m*-C_6H_4, *J* (HH) = 8 Hz), 8.06 (s, 2H, CH). $^{13}C\{^1H\}$ NMR (75.5 MHz, CD_3CN, r. t.): δ 21.0 (CH_3), 65.0 (CH_2, C_5H_4 or C═N), 69.4 (CH_2, C_5H_4 or C═N), 71.3 (CH_2, C_5H_4 or C═N), 81.4 (CH_2, C_5H_4 or C═N), 127.9 (C_6H_4), 129.1 (C_6H_4), 136.3 (C_6H_4), 136.4 (C_6H_4), 161.1 (C_6H_4). mp: 113−116 °C. Figure 10 shows the molecular structure determined by X-ray crystallography.

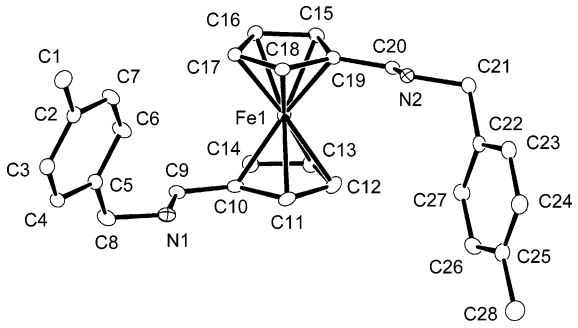

Figure 10. ORTEP drawing of 1,1′-bis(*p*-xylyliminomethyl)ferrocene with 50% ellipsoidal plotting.

Preparation of 1,1′-Bis(*p*-xylylaminomethyl)ferrocene (3). 1,1′-Bis(*p*-xylyliminomethyl)ferrocene (1.42 g, 3.17 mmol) was dissolved in a THF/MeOH solution (THF/MeOH = 50 mL:50 mL). $NaBH_4$ (360 mg, 9.52 mmol) was added to the solution and stirred for 2 h at room temperature. An extra portion of $NaBH_4$ (360 mg, 9.52 mmol) was added to the reaction mixture, which was stirred for further 24 h, before being quenched with 1 N HCl (100 mL). Evaporation of the solvent gave the remaining solid, which was partitioned between 2 N KOH and CH_2Cl_2. The organic extract was dried over $MgSO_4$ then filtered and concentrated under reduced pressure to give **3** as brown oil (1.42 g, 99%). Anal. Calcd. for $C_{28}H_{32}N_2Fe$: C, 74.33; H, 7.13; N, 6.19. Found: C, 74.07; H, 7.39; N, 5.91. ^{1}H NMR (300 MHz, $CDCl_3$, r. t.): δ 2.33 (s, 6H, CH_3), 3.47 (s, 4H, CH_2), 3.74 (s, 4H, CH_2), 4.03 (m, 4H, C_5H_4), 4.10 (m, 4H, C_5H_4), 7.12 (d, 4H, *o*-C_6H_4 or *m*-C_6H_4, *J* (HH) = 8 Hz), 7.20 (t, 4H, *o*-C_6H_4 or *m*-C_6H_4, *J*(HH) = 8 Hz). $^{13}C\{^1H\}$ NMR (75.5 MHz, $CDCl_3$, r. t.): δ 21.0 (CH_3), 47.8 (CH_2), 52.9 (CH_2), 68.1 (C_5H_4), 68.6 (C_5H_4), 86.9 (C_5H_4), 127.9 (C_6H_4), 129.0 (C_6H_4), 136.3 (C_6H_4), 137.1 (C_6H_4).

Preparation of [1−H]$^+$(PF_6). A suspension of **1** (362 mg, 1.13 mmol) in 6 N HCl (40 mL) was stirred for 12 h at room temperature. Evaporation of the solvent gave [**1**−H]$^+$Cl, which was washed with water. To a suspension of [**1**−H]$^+$Cl in acetone (50 mL) was added NH_4PF_6 (1.63 g, 10 mmol), and the mixture was stirred for 4 h at room temperature. The precipitate was removed by filtration. Evaporation of the filtrate gave [**1**−H]$^+$(PF_6) as a yellow solid (408 mg, 0.877 mmol, 78%). Anal. Calcd. for $C_{19}H_{22}NF_6FeP$: C, 49.06; H, 4.77; N, 3.01. Found: C, 48.98; H, 4.65; N, 3.02. ^{1}H NMR (300 MHz, CD_3CN, r. t.): δ 2.34 (s, 3H, CH_3), 4.04 (br, 2H, CH_2), 4.06 (br, 2H, CH_2), 4.21 (s, 5H, C_5H_5), 4.28 (m, 2H, C_5H_4), 4.37 (m, 2H, C_5H_4), 7.25 (d, 2H, C_6H_4, *J* (HH) = 8 Hz), 7.30 (d, 2H, C_6H_4, *J* (HH) = 8 Hz). $^{13}C\{^1H\}$ NMR spectrum (75.5 MHz, CD_3CN, r. t.): δ 21.3 (CH_3), 48.7 (CH_2), 51.6 (CH_2), 70.1 (C_5H_5 or C_5H_4), 70.7 (C_5H_5 or C_5H_4), 71.7 (C_5H_5 or C_5H_4), 76.5 (C_5H_5 or C_5H_4), 128.4 (C_6H_4), 130.6 (C_6H_4), 131.0 (C_6H_4), 140.6 (C_6H_4). IR spectrum (KBr): ν (N−H), 3266 and 3233 cm^{-1}. mp: 189−192 °C (decomp).

Preparation of [2−H]$^+$(PF_6). A suspension of **2** (740 mg, 2.47 mmol) in 6 N HCl (60 mL) was stirred for 12 h at room temperature. Evaporation of the solvent gave [**2**−H]$^+$Cl, which was washed with water. To a suspension of [**2**−H]$^+$Cl in acetone (50 mL) was added NH_4PF_6 (1.63 g, 10 mmol), and the mixture was stirred for 4 h at room temperature. The precipitate was removed by filtration, and the evaporation of the filtrate gave [**2**−H]$^+$(PF_6) as a yellow solid (395 mg, 0.887 mmol, 36%). Anal. Calcd. for $C_{17}H_{26}NF_6FeP$: C,

Table 1. Crystal Data and Details of Structure Refinement of $[(DB24C8)(1\text{-}H)]^+(PF_6)$ and $[(DB24C8)_2(3\text{-}H_2)]^{2+}(PF_6)_2$ and 1,1′-Bis(*p*-xylyliminomethyl)ferrocene (Fc-imine)

compound	$[(DB24C8)(\mathbf{1}-H)]^+(PF_6)$	$[(DB24C8)_2(\mathbf{3}-H_2)]^{2+}(PF_6)_2(H_2O)_2$	Fc-imine
formula	$C_{43}H_{54}F_6FeNO_8P$	$C_{76}H_{102}FeN_2P_2F_{12}O_{18}$	$C_{28}H_{28}FeN_2$
mol wt	913.71	1677.42	448.39
cryst syst	triclinic	triclinic	monoclinic
space group	$P\bar{1}$ (No. 2)	$P\bar{1}$ (No. 2)	$P2_1/c$ (No. 14)
a/Å	10.1889(13)	10.568(7)	5.9651(11)
b/Å	11.050(3)	18.641(12)	13.627(2)
c/Å	19.460(2)	22.41(2)	27.819(8)
α/deg	87.09(3)	78.21(3)	
β/deg	98.43(2)	82.02(3)	102.955(12)
γ/deg	89.02(2)	69.27(2)	
V/Å^3	2135.1(7)	4032(5)	2203.7(8)
Z	2	2	4
μ (Mo Kα)/cm^{-1}	4.69	3.22	7.02
F(000)	956.00	1760.00	944.00
D c/g cm^{-1}	1.421	1.382	1.351
crystal size/mm	0.5 × 0.2 × 0.15	0.3 × 0.1 × 0.1	0.5 × 0.2 × 0.2
unique reflns	8838	16527	4909
used reflns [$I \geq 3.0\sigma(I)$]	5174	6515	3355
no. of variables	595	1088	308
R	0.063	0.111	0.037
R_w	0.090	0.138	0.050
GOF	0.95	1.34	1.00

45.86; H, 5.89; N, 3.15. Found: C, 45.98; H, 6.03; N, 3.20. ^{1}H NMR (300 MHz, CD_3CN, r. t.): δ 0.88 (t, 3H, CH_3, *J* (HH) = 7 Hz), 1.28−1.32* (6H, CH_2), 1.57 (m, 2H, CH_2), 2.90 (m, 2H, NCH_2-CH_2), 3.97 (s, 2H, $NCH_2C_5H_4$), 4.20 (s, 5H, C_5H_5), 4.27 (m, 2H, C_5H_4), 4.35 (m, 2H, C_5H_4), 6.41 (br, 2H, NH_2). ^{13}C{^{1}H} NMR (75.5 MHz, CD_3CN, r. t.): δ 14.2 (CH_3), 23.0 (CH_2), 26.3 (CH_2), 26.5 (CH_2), 31.7 (CH_2), 48.2 (NCH_2), 48.7 (NCH_2), 69.9 (C_5H_5 or C_5H_4), 70.5 (C_5H_5 or C_5H_4), 71.3 (C_5H_5 or C_5H_4), 76.6 (C_5H_5 or C_5H_4). The peak with asterisk is overlapped significantly with other signals. mp: 193−196 °C (decomp).

Preparation of $[\mathbf{3}-H_2]^{2+}(PF_6)_2$. A heterogeneous solution of 1,1′-bis(*p*-xylylaminomethyl)ferrocene (**3**) (460 mg, 1.02 mmol) in 6 N HCl (50 mL) was stirred for 13 h at room temperature. Evaporation of the solvent gave $[\mathbf{3}-H_2]^{2+}Cl_2$ that was washed with water. $[\mathbf{3}-H_2]^{2+}Cl_2$ was suspended in an acetone solution (50 mL) of NH_4PF_6 (1.65 g, 10 mmol), and the suspension was stirred for 4 h at room temperature. The precipitate was removed by the filtration and the evaporation of the filtrate gave $[\mathbf{3}-H_2]^{2+}(PF_6)_2$ as a yellow solid (523 mg, 0.703 mmol, 69%). Anal. Calcd. for $C_{28}H_{34}NF_{12}Fe_2P_2$: C, 45.18; H, 4.60; N, 3.76. Found: C, 45.40; H, 4.53; N, 3.76. ^{1}H NMR (300 MHz, CD_3CN, r. t.): δ 2.35 (s, 6H, CH_3), 4.03 (m, 4H, CH_2), 4.07 (m, 4H, CH_2), 4.32 (m, 4H, C_5H_4), 4.41 (m, 4H, C_5H_4,), 6.78 (br, 4H, NH_2), 7.27 (m, 4H, *o*-C_6H_4 or *m*-C_6H_4), 7.29 (m, 4H, *o*-C_6H_4 or *m*-C_6H_4). ^{13}C{^{1}H} NMR (75.5 MHz, CD_3CN, r. t.): δ 21.3 (CH_3), 48.3 (CH_2), 51.8 (CH_2), 71.7 (br, C_5H_4), 72.6 (br, C_5H_4), 77.5 (C_5H_4), 128.5 (C_6H_4), 130.6 (C_6H_4), 131.0 (C_6H_4), 140.8 (C_6H_4). ^{13}C{^{1}H} NMR (100 MHz, CD_3CN, 60 °C): δ 21.4 (CH_3), 48.7 (CH_2), 52.2 (CH_2), 72.1 (C_5H_4), 72.7 (C_5H_4), 77.9 (C_5H_4), 128.7 (C_6H_4), 130.9 (C_6H_4), 131.1 (C_6H_4), 141.1 (C_6H_4). mp: 197−200 °C (decomp).

Isolation of $[(DB24C8)(\mathbf{1}-H)]^+(PF_6)$. Yellow crystals of pseudorotaxane $[(DB24C8)(\mathbf{1}-H)]^+(PF_6)$ were obtained by vapor diffusion of Et_2O into a solution of $[\mathbf{1}-H]^+(PF_6)$ (58.3 mg) and DB24C8 (46.5 mg) in CH_2Cl_2 (2 mL) in 72% yield. $[(DB24C8)(\mathbf{1}-H)]^+(PF_6)$ was obtained in 72% yield. Anal. Calcd. for $C_{43}H_{54}NF_6FeP$: C, 56.52; H, 5.96; N, 1.53. Found: C, 56.37; H, 5.80; N, 1.53. IR (KBr): ν(N−H), 3067 and 3166 cm^{-1}. FABMS: *m*/*z* = 768 $[M - PF_6]^+$.

[2]Pseudorotaxane Formation in CD_3CN. In an NMR tube was charged a CD_3CN solution (0.7 mL) of DB24C8 (3.1 mg, 0.0069 mmol) and the ammonium salts ($[\mathbf{1}-H]^+(PF_6)$ 3.3 mg, 0.0070 mmol, or $[\mathbf{2}-H]^+(PF_6)$, 3.1 mg, 0.0070 mmol). The sample was placed in an NMR spectrometer. The ^{1}H NMR spectra were recorded at 30 °C. The molar ratio of DB24C8 and ammonium salts was determined by comparison of the peak area of methylene hydrogens.

^{1}H NMR of $[(DB24C8)(\mathbf{1}-H)]^+(PF_6)$ (300 MHz, CD_3CN, r. t.): δ 2.14 (s, 3H, CH_3), 3.60−4.20* (OCH_2, C_5H_5, C_5H_4, 33H), 4.37 (m, 2H, NCH_2), 4.53 (m, 2H, NCH_2), 6.85−6.64* (10H, C_6H_4, *o*- or *m*-C_6H_4 (DB24C8)), 7.14 (2H, *o*- or *m*-C_6H_4 (DB24C8)). ^{1}H NMR of $[(DB24C8)(\mathbf{2}-H)]^+(PF_6)$ (400 MHz, CD_3CN, 30 °C): δ 0.89 (t, 3H, CH_3, *J* (HH) = 1 Hz), 1.03−1.11* (4H, CH_2), 1.29−1.38* (2H, CH_2), 1.40 (m, 2H, CH_2), 3.32 (m, 2H, NCH_2), 3.60−4.35* (35H, C_5H_5, OCH_2), 6.88−6.98* (8H, C_6H_4). FABMS: *m*/*z* = 748 $[M - PF_6]^+$. The peaks with asterisks are overlapped significantly with other signals.

[2] and [3]Pseudorotaxane Formation in CD_3CN. DB24C8 (3.1 mg, 0.0069 mmol) and $[\mathbf{3}-H_2]^{2+}(PF_6)_2$ (5.2 mg, 0.0070 mmol) were dissolved in CD_3CN (0.7 mL) in an NMR tube. The molar ratio of $[\mathbf{3}-H_2]^{2+}(PF_6)_2$, $[(DB24C8)(\mathbf{3}-H_2)]^{2+}(PF_6)_2$, and $[(DB24C8)_2(\mathbf{3}-H_2)]^{2+}(PF_6)_2$ in the reaction mixture was determined to be 4.0:4.2:1.1 by the ^{1}H NMR spectrum (CH_2 peak area ratio). Evaporation of the solvent left a red solid whose FABMS spectrum showed the peaks of the [2] and [3]pseudorotaxanes. The solution from DB24C8 (3.1 mg, 0.0069 mmol) and $[\mathbf{3}-H_2]^{2+}(PF_6)_2$ (15.7 mg, 0.0035 mmol) in CD_3CN (0.7 mL) contained [3]pseudorotaxane, $[(DB24C8)_2(\mathbf{3}-H_2)]^{2+}(PF_6)_2$, only. ^{1}H NMR of $[(DB24C8)(\mathbf{3}-H_2)]^{2+}(PF_6)_2$ (400 MHz, CD_3CN, r. t.): δ 2.15 (s, 3H, CH_3), 2.34−2.36* (3H, CH_3), 3.53−4.25* (32H, C_5H_4, NCH_2, OCH_2), 4.21 (m, 2H, C_5H_4), 4.27 (m, 2H, C_5H_4), 4.38 (m, 2H, NCH_2), 4.56 (m, 2H, NCH_2), 6.87−6.92* (12H, C_6H_4), 7.14 (2H, C_6H_4 (DB24C8), *J*(HH) = 8 Hz), 7.26−7.29* (4H, C_6H_4 (DB24C8)). NH_2 was not observed. FABMS: *m*/*z* = 1047 $[M - PF_6]^+$. ^{1}H NMR of $[(DB24C8)_2(\mathbf{3}-H_2)]^{2+}(PF_6)_2$ (400 MHz, CD_3CN, r. t.): δ 2.16 (s, 6H, CH_3), 3.53−4.11*(68H, C_5H_4, OCH_2), 3.96 (m, C_5H_4, 4H), 4.21 (m, NCH_2, 4H), 4.48 (m, NCH_2, 4H), 6.86−6.93* (20H, C_6H_4), 7.14 (br, 4H, NH_2), 7.15 (4H, C_6H_4 (DB24C8), *J* (HH) = 8 Hz). FABMS: *m*/*z* = 1496 $[M - PF_6]^+$, 901 $[M - 2(PF_6)]^+$. The peaks with asterisks are overlapped significantly with other signals.

Spectroscopic Measurement of Electrochemical Formation of [2]Pseudorotaxane. A typical kinetic experiment is as follows. A CH_3CN solution of **1** (2.0 mM) containing *n*-Bu_4NPF_6 (0.1 M)

was electrochemically oxidized at 0.4 V (vs Ag^+/Ag) by using flow electrolysis system and was soon collected to a 1 cm × 1 cm quartz cell. After addition of DB24C8 (0, 4, 10, 20, or 40 mM) to the solution, the absorption spectra were measured every 3 min.

Crystal Structure Analysis. Crystals of $[(DB24C8)(\mathbf{1}-H)]^+(PF_6)$, $[(DB24C8)_2(\mathbf{3}-H_2)]^{2+}(PF_6)_2$, and 1,1′-bis{(4-xylyl)iminomethyl}ferrocene suitable for X-ray diffraction study were obtained by recrystallization from CH_2Cl_2/Et_2O, CH_2Cl_2/acetone/*n*-Pr_2O, and Et_2O, respectively, and mounted in glass capillary tubes. The data were collected to a maximum 2θ value of 55.0°. A total of 720 oscillation images were collected. A sweep of data was done using ω scans from −110.0° to 70.0° in 0.5° steps, at $\chi = 45.0°$ and $\phi = 0.0°$. The detector swing angle was −20.42°. A second sweep was performed using ω scans from −110.0° to 70.0° in 0.5° step, at $\chi = 45.0°$ and $\phi = 90.0°$. The crystal-to-detector distance was 44.84 mm. Readout was performed in the 0.070 mm pixel mode. Calculations were carried out by using a program package Crystal Structure for Windows.[27] The structure was solved by direct methods and expanded using Fourier techniques. A full-matrix least-squares refinement was used for the nonhydrogen atoms withanisotropic thermal parameters. Crystal data and detailed results of refinement are summarized in Table 1.

Acknowledgment. This work was financially supported by a Grant-in-aid for Scientific Research from the Ministry of Education, Culture, Sport, Science, and Technology Japan, and by The 21st Century COE Program "Creation of Molecular Diversity and Development of Functionalities". We are grateful to Assistant Prof. Atsushi Mori of our institute for FABMS measurement.

Supporting Information Available: Crystallographic data have been deposited at the CCDC, 12 Union Road, Cambridge CB21EZ, UK and copies can be obtained on request, free of charge, by quoting the publication citation and the deposition numbers, 235382, 257706, and 257707.

IC050215F

(27) *Crystal Structure 3.6.0: Crystal analysis package, Rigaku and Rigaku/MSC* (2000−2004).